Agonist *Versus* Antagonist Action of ATP at the P2Y$_4$ Receptor Is Determined by the Second Extracellular Loop[*]

Christopher L. Herold, **Ai-Dong Qi**, **T. Kendall Harden**, and **Robert A. Nicholas**[‡]
Department of Pharmacology, University of North Carolina, Chapel Hill, North Carolina 27599-7365

Abstract

UTP is a potent full agonist at both the human P2Y$_4$ (hP2Y$_4$) and rat P2Y$_4$ (rP2Y$_4$) receptor. In contrast, ATP is a potent full agonist at the rP2Y$_4$ receptor but is a similarly potent competitive antagonist at the hP2Y$_4$ receptor. To delineate the structural determinants of agonism *versus* antagonism in these species homologues, we expressed a series of human/rat P2Y$_4$ receptor chimeras in 1321N1 human astrocytoma cells and assessed the capacity of ATP and UTP to mobilize intracellular Ca^{2+}. Replacement of the NH$_2$ terminus of the hP2Y$_4$ receptor with the corresponding region of the rP2Y$_4$ receptor resulted in a receptor that was activated weakly by ATP, whereas replacement of the second extracellular loop (EL2) of the hP2Y$_4$ receptor with that of the rP2Y$_4$ receptor yielded a chimeric receptor that was activated fully by UTP and near fully by ATP, albeit with lower potencies than those observed at the rP2Y$_4$ receptor. These potencies were increased, and ATP was converted to a full agonist by replacing both the NH$_2$ terminus and EL2 in the hP2Y$_4$ receptor with the corresponding regions from the rP2Y$_4$ receptor. Mutational analysis of the five divergent amino acids in EL2 between the two receptors revealed that three amino acids, Asn-177, Ile-183, and Leu-190, contribute to the capacity of EL2 to impart ATP agonism. Taken together, these results suggest that the second extracellular loop and the NH$_2$ terminus form a functional motif that plays a key role in determining whether ATP functions as an agonist or antagonist at mammalian P2Y$_4$ receptors.

Extracellular nucleotides elicit diverse physiological effects by activating G protein-coupled P2Y receptors (1,2). Molecular cloning and heterologous receptor expression studies have led to the identification and characterization of eight human P2Y (hP2Y)1 receptor subtypes (hP2Y$_{1,2,4,6,11-14}$). hP2Y$_1$, hP2Y$_2$, hP2Y$_4$, hP2Y$_6$, and hP2Y$_{11}$ receptors display 27–52% amino acid identity and couple via heterotrimeric G proteins of the G$_q$ family to the activation of phospholipase C, generation of inositol phosphates, and mobilization of intracellular Ca^{2+} stores (2–4). In addition to coupling to phospholipase C, the hP2Y$_{11}$ receptor also couples to G$_s$ to activate adenylyl cyclase and promotes cyclic AMP accumulation (5–7). The recently identified P2Y$_{12}$, P2Y$_{13}$, and P2Y$_{14}$ receptors, which are encoded on a short segment of chromosome 3, have high sequence identity with each other (40–48%) but share relatively little sequence identity (22–25%) with the other hP2Y receptors. The P2Y$_{12}$ receptor has been shown to be the G$_i$-coupled receptor in platelets that, together with the P2Y$_1$ receptor, mediate ADP-promoted platelet aggregation (8–11). P2Y$_{13}$ and P2Y$_{14}$ receptors are also coupled to G$_i$ and are activated by ADP and UDP-glucose, respectively (12,13).

Differences in nucleotide selectivity have been observed between species orthologues of P2Y receptors. For example, the avian p2y3 and rat P2Y$_6$ receptor are species homologues with ~65% identity that differ in their capacity to mediate adenine nucleotide-promoted inositol

phosphate accumulation (14). Whereas UDP and UTP have similar potencies at the two receptors, ADP and ATP are considerably more potent and efficacious at the avian p2y3 receptor than at the rat $P2Y_6$ receptor. Human and canine $P2Y_{11}$ receptors, which share ~70% amino acid identity (15), also differ in their ability to be activated by adenine nucleotides. ATP nucleotides are more potent and efficacious than their corresponding diphosphate nucleotides at the human $P2Y_{11}$ receptor for promotion of both inositol phosphate and cAMP accumulation, whereas ADP nucleotides are considerably more potent than their corresponding triphosphates at the canine $P2Y_{11}$ receptor (16).

We have also observed a remarkable difference in the nucleotide selectivities and agonism *versus* antagonism between rat and human $P2Y_4$ receptors, which exhibit 83% sequence identity (17). Under conditions that minimized confounding factors such as nucleotide metabolism, bioconversion, and endogenous nucleotide release, UTP, ATP, diadenosine tetraphosphate, ITP, GTP, CTP, and XTP were all full agonists at the $rP2Y_4$ receptor, whereas only UTP, GTP, and ITP activated the $hP2Y_4$ receptor. Moreover, whereas ATP acted as a potent, full agonist at the $rP2Y_4$ receptor, it was a similarly potent competitive antagonist at the $hP2Y_4$ receptor.

The capacity of ATP to bind with relatively high affinity to both species homologues of the $P2Y_4$ receptor, but to act as an agonist at one receptor and an antagonist at the other, provides an ideal signaling system to pursue the structural basis of agonism *versus* antagonism. A series of $hP2Y_4/rP2Y_4$ receptor chimeras was constructed, and we report here that the second extracellular loop (EL2) of the $P2Y_4$ receptor is a major determinant of agonist *versus* antagonist activity of ATP, whereas the NH_2 terminus plays a lesser role. Moreover, 3 amino acids from EL2 of the $hP2Y_4$ receptor, when replaced with the corresponding residues from the $rP2Y_4$ receptor, are sufficient to convert ATP from an antagonist to nearly a full agonist at the $hP2Y_4$ receptor. These studies implicate the EL2 of the $P2Y_4$ receptor, and possibly other P2Y receptors, as a major mediator of receptor activation.

EXPERIMENTAL PROCEDURES

Materials

All tissue culture reagents and Hanks' balanced salt solution (HBSS) were supplied by either Mediatech, Inc. (Herndon, VA) or the Lineberger Comprehensive Cancer Center tissue culture facility (University of North Carolina, Chapel Hill, NC). ATP and UTP (AP Biotech, Piscataway, NJ) were at least 99% pure and contained no other contaminating nucleotides. Fura-2/AM was from Molecular Probes (Eugene, OR). Polybrene and sodium butyrate were from Sigma Chemical (St. Louis, MO). Mouse HA.11 monoclonal antibody was from BAbCO (Richmond, CA). [^{125}I]Rabbit anti-mouse IgG (0.1 μCi/ml) was from PerkinElmer Life Sciences (Boston, MA). *Pfu* polymerase was from Stratagene (La Jolla, CA).

Site-directed Mutagenesis and Construction of Chimeric Receptors

$hP2Y_4/rP2Y_4$ chimeras and receptors harboring point mutations were generated by four primer PCR (18). PCR amplification with overlapping primers was carried out with *Pfu* DNA polymerase from 1 ng of template. The amplification conditions were: 94 °C for 5 min; 35 cycles of 94 °C for 30 s, 56 °C for 30 s, and 72 °C for 75 s; and a final extension for 7 min at 72 °C. To generate chimera 1/EL2, chimera 1 DNA was used as a template along with specific primer pairs.

Chimeric and mutant receptor DNA constructs created as described above were digested with EcoRI and XhoI and ligated into similarly digested pLXSN vector (19). Receptors harboring the influenza virus hemagglutinin (HA) epitope tag at their NH_2 termini were constructed by

amplifying the coding sequence of receptors with an upstream primer containing an MluI site just preceding the second codon. The amplified fragments were digested with MluI and XhoI and used to replace the coding sequence of the human $P2Y_1$ receptor in the plasmid pLXSN-HA-$hP2Y_1$, which contained 15 bp of 5′-untranslated sequence, the initiating ATG codon, and the HA tag sequence followed by an MluI site at the start of the human $P2Y_1$ receptor coding sequence. Addition of an HA tag at the NH_2 terminus of a G protein-coupled receptor has been shown to have no effect on its pharmacological selectivity (20,21). Receptor constructs were sequenced at the University of North Carolina, Chapel Hill Automated DNA Sequencing Facility.

Expression of Receptors in 1321N1 Human Astrocytoma Cells

Receptors were expressed in 1321N1 cells by using the retroviral expression system described by Comstock *et al.* (22). Briefly, pLXSN retroviral plasmids containing the appropriate receptor sequence were transfected into the murine packaging cell line PA317 by calcium phosphate precipitation. Following a 2-day incubation at 32 °C in the presence of 5 mM sodium butyrate, the virus-containing medium was collected, filtered, and incubated with 1321N1 human astrocytoma cells for 2 h in the presence of 8 μg/ml Polybrene. Infected 1321N1 cells were selected for Geneticin resistance for 10–14 days in the presence of 1 mg/ml G-418.

Cell Culture

PA317 cells were grown in DMEM-H, 10% fetal bovine serum, 100 units/ml penicillin, and 0.1 mg/ml streptomycin. 1321N1 cells stably expressing receptors were grown in DMEM-H, 5% fetal bovine serum, 0.4 mg/ml G-418, 100 units/ml penicillin, 0.1 mg/ml streptomycin, and 0.25 μg/ml amphotericin B. Cells were grown in monolayer and maintained at 37 °C in a humidified atmosphere of 5% CO_2/95% air.

Intracellular [Ca^{2+}] Measurements

Intracellular [Ca^{2+}] was determined as described previously (16,17). Briefly, cells were grown on 22-mm glass coverslips to ~20% confluence and then were loaded with 750 nM Fura-2/AM for 30 min. Coverslips were encased in a Plexiglas flowthrough chamber (0.2-ml volume) and continuously superfused at ~1.4 ml/min with buffer (HBSS plus Ca^{2+}/Mg^{2+}) with or without ligands. The chamber was secured to the stage of a Nikon inverted fluorescence microscope, and data were recorded and processed with an InCyt Im2 imaging system (Intracellular Imaging Inc., Cincinnati, OH). Ligands were applied for 30 s, and intracellular [Ca^{2+}] was monitored in 6–15 individual cells per coverslip. A small number of unresponsive cells that were not activated by a maximal dose of UTP (100–300 μM) were not included for analysis. To generate concentration-response curves, each concentration of nucleotide was applied only once to each coverslip to avoid receptor desensitization, and the area under the curve (AUC) was determined by using National Institutes of Health Image software. The values from at least three coverslips were averaged and plotted as a function of nucleotide concentration.

Radioimmunoassay

Cells were seeded in 24-well plates at 5×10^4 cells/well 3 days prior to assay. Cells were fixed with 0.2 ml of 4% paraformaldehyde for 30 min at room temperature, washed twice with 1 ml of HBSS plus Ca^{2+}/Mg^{2+}, and blocked for 30 min at room temperature with 0.2 ml of DMEM-H plus 50 mM HEPES, pH 7.1, and 10% fetal bovine serum. Cells were incubated with mouse HA.11 monoclonal antibody at a 1:1000 dilution in 0.2 ml of medium for 1 h at room temperature. Following two washes with 1 ml of HBSS plus Ca^{2+}/Mg^{2+}, cells were incubated with [^{125}I]rabbit anti-mouse IgG antibody diluted to 1:500 in 0.2 ml of medium for 2 h at room temperature. Following another series of washing steps, cells were solubilized in 0.4 ml of 1 M NaOH overnight and transferred to glass tubes for quantitation in a gamma counter.

Data Analysis and Statistics

EC_{50} values and 95% confidence limits for EC_{50} values were calculated by non-linear regression with Graph-Pad Prism 3.0 software (GraphPad, San Diego, CA). Data were compared using one-way analysis of variance and Tukey's post-test comparison, with $p < 0.05$ considered to be statistically significant.

RESULTS

Construction of Chimeric $hP2Y_4$ and $rP2Y_4$ Receptors

We previously reported that ATP is a potent full agonist at the $rP2Y_4$ but is a similarly potent competitive antagonist at the $hP2Y_4$ (17). To ascertain the structural basis for this difference in agonism *versus* antagonism, we generated a series of chimeric receptors between these similar species orthologues (83% identity; see Fig. 1*A*). As illustrated in Fig. 1*B*, these chimeras were constructed by systematic replacement of small regions of the $hP2Y_4$ with the corresponding regions from the $rP2Y_4$ receptor. The replacements were made in the $hP2Y_4$ receptor so we could identify one or more domains from the $rP2Y_4$ receptor that conferred a change of ATP from a potent antagonist to a potent agonist when inserted into the $hP2Y_4$ receptor. Thus, these experiments were designed to identify a "gain of function" by analyzing the responsiveness of the chimeric receptors to ATP. The receptors were stably expressed in 1321N1 human astrocytoma cells, which do not exhibit functional responses to extracellular nucleotides (23), and nucleotide-promoted intra-cellular Ca^{2+} mobilization was quantitated under conditions that minimized the potential confounding effects of nucleotide metabolism, bioconversion, and accumulation of released nucleotides (17).

As previously studied in detail (17), 100 μM ATP failed to activate the $hP2Y_4$ receptor, whereas application of 100 μM UTP to $hP2Y_4$-1321N1 cells induced a rapid, reversible rise in intracellular Ca^{2+} levels (Fig. 2*A*, *right panel*). This profile was clearly different from that of the $rP2Y_4$ receptor, which displayed robust responses to both ATP and UTP (Fig. 2*B*, *right panel*). The lower apparent maximum effect of UTP compared with ATP illustrated in the *right panel* in Fig. 2*B* was due to desensitization of the $rP2Y_4$, because the maximum increase in intracellular $[Ca^{2+}]$ evoked by a single application of 100 μM ATP or UTP applied to separate coverslips was identical (Fig. 2*B*, *left panel* and data not shown).

Concentration-response curves for nucleotides were generated by integrating the area under the curve (AUC) of the Ca^{2+} response averaged from 6–15 cells on a coverslip, with at least three coverslips assayed for each concentration. To avoid concerns about desensitization, each coverslip was exposed only once to a single nucleotide concentration. AUC values for each agonist concentration reflect both the time and magnitude of the Ca^{2+} mobilization response and the number of responding cells in the imaging field. UTP increased intracellular Ca^{2+} levels in 1321N1-$hP2Y_4$ cells with an EC_{50} of 530 ± 220 nM, whereas ATP was without agonist effect at all concentrations tested (Fig. 2*A*, *left panel*, and Table I). Moreover, ATP competitively antagonized the stimulatory effects of UTP at the $hP2Y_4$ with a K_b value (antagonist dissociation constant) of 700 nM that is very similar to the potency of UTP for activation (Ref. 17 and data not shown). In contrast, both UTP and ATP promoted intracellular Ca^{2+} mobilization in 1321N1-$rP2Y_4$ cells with EC_{50} values of 600 ± 220 and 890 ± 460 nM, respectively (Fig. 2*B*, *left panel*, and Table I). Thus, UTP activated both the $hP2Y_4$ and $rP2Y_4$ receptor with comparable potencies, whereas ATP was a full agonist at the $rP2Y_4$ receptor and an antagonist at the $hP2Y_4$ receptor.

Characterization of the $hP2Y_4$/$rP2Y_4$ Receptor Chimeras

Each of the seven first-generation chimeras (Fig. 1*B*) was fully functional when expressed in 1321N1 cells, with UTP promoting robust intracellular Ca^{2+} mobilization responses (Fig. 3

and Table I). The EC_{50} values for UTP ranged from 0.55 to 13 μM for the various constructs (Table I). However, marked differences in the response to ATP were observed among the chimeras. Similar to the $hP2Y_4$ receptor, no responses to 100 μM ATP were observed in 1321N1 cells expressing chimeras 2, 3, 5, 6, or 7 (Fig. 3*B* and data not shown). A weak but reproducible response to ATP was observed with chimera 1 (Fig. 3*A*). However, a nearly full agonist response to ATP was observed in cells expressing chimera 4, which contained the second intra-cellular loop (IL2), transmembrane 4 (TM4), and the second extracellular loop (EL2) of the $rP2Y_4$ receptor (Fig. 3*C*). The EC_{50} values of UTP and ATP at chimera 4 were 13 and 95 μM, respectively (Table I). The reason(s) for the shift to the right of the agonist activation curves in chimera 4 but not in the other chimeras has not been fully pursued, but it is unlikely that it is due to differences in receptor expression at the cell surface (as discussed below). These data demonstrate that the region encompassing the second intracellular loop and second extracellular loop of the $hP2Y_4$ and $rP2Y_4$ receptors is a uniquely important determinant of ATP agonism at the $P2Y_4$ receptor.

Roles of IL2, TM4, and EL2 from the rat $P2Y_4$ Receptor in Imparting ATP Agonist Activity to the Human $P2Y_4$ Receptor

The results with chimera 4 suggested the existence of identifiable sequence in the $P2Y_4$ receptor responsible for agonist *versus* antagonist action of ATP. Thus, we generated two additional chimeras, in which IL2 and TM4 (chimera 4A) or EL2 (chimera 4/EL2) of the $hP2Y_4$ receptor were replaced individually with their cognate sequences from the $rP2Y_4$ receptor (see Fig. 1*A*). As was observed with chimeras 1–7, UTP was a potent agonist at these chimeric $P2Y_4$ receptors (Fig. 4 and Table I). Replacement of IL2 and TM4 of the $hP2Y_4$ receptor with the corresponding region from the $rP2Y_4$ receptor failed to alter the phenotype of the $hP2Y_4$ receptor (Fig. 4*A*), whereas replacement of EL2 of the $hP2Y_4$ receptor with the corresponding domain from the $rP2Y_4$ receptor resulted in a near full agonist response to ATP (Fig 4*B*). Moreover, the agonist profile of chimera 4/EL2 was essentially identical to that of chimera 4 (Table I). These data indicate that EL2 specifies the ability of ATP to act as an agonist or antagonist at the $P2Y_4$ receptor.

As illustrated earlier, replacement of the $hP2Y_4$ receptor NH_2 terminus with the corresponding sequence from the $rP2Y_4$ receptor (chimera 1) resulted in a receptor that was activated, albeit weakly, by 100 μM ATP (Fig. 3*A*). Therefore, we constructed an additional chimera of the $hP2Y_4$ receptor (chimera 1/EL2), in which both the NH_2 terminus and EL2 of the $hP2Y_4$ receptor were replaced by the cognate regions from the $rP2Y_4$ receptor, with the goal of generating a $P2Y_4$ receptor exhibiting potencies for UTP and ATP more closely resembling those of the wild type $rP2Y_4$ receptor. Indeed, the EC_{50} values of UTP and ATP for promotion of intracellular Ca^{2+} mobilization at chimera 1/EL2 were 1.9 and 12 μM, respectively (Fig. 4*C* and Table I). Moreover, ATP became an apparent full agonist at chimera 1/EL2, compared with the partial agonism of ATP in chimera 4/EL2 (Fig. 4, compare *B* with *C*). Thus, the incorporation of the $rP2Y_4$ NH_2 terminus onto chimera 4 increased the potencies of UTP and ATP 4- to 5-fold and converted ATP to an apparent full agonist, suggesting that the $rP2Y_4$ NH_2 terminus is a minor determinant of the agonist activity of ATP at the $rP2Y_4$ receptor.

Roles of Individual Amino Acids in EL2 of the Rat $P2Y_4$ Receptor in Imparting Agonist Activity to ATP

Because EL2 was a major determinant of agonist *versus* antagonist activity at the two $P2Y_4$ receptor homologues, we individually mutated each of the 5 divergent amino acids (Fig. 1*A*) in EL2 of the $hP2Y_4$ receptor to the corresponding residue of the $rP2Y_4$ receptor. Cells stably expressing these $hP2Y_4$ receptor point mutants exhibited robust Ca^{2+} responses to UTP (Fig. 5), and the potencies of UTP at the mutant $hP2Y_4$ receptors were very similar to that at the wild type $hP2Y_4$ receptor (Table I). ATP was not an agonist in cells expressing the $hP2Y_4$-

N178A and hP2Y$_4$-K179N mutants. In contrast, introduction of single point mutations at Ser-177 (S177N), Val-183 (V183I), and Arg-190 (R190L) resulted in P2Y$_4$ receptors at which ATP was active, albeit with much lower efficacies and potencies than those observed in chimera 4/EL2 (Fig. 5). The EC$_{50}$ values for ATP-promoted intracellular Ca^{2+} mobilization at these hP2Y$_4$ mutant receptors could not be determined, because the concentration-response curves for ATP did not reach a maximum at less than millimolar concentrations. To determine if these three residues were the only determinants of ATP agonism in EL2, we mutated Ser-177, Val-183, and Arg-190 together to the corresponding residues of the rP2Y$_4$ receptor (triple mutant) and generated concentration-response curves to ATP. The triple mutant receptor had essentially identical EC$_{50}$ values for both UTP and ATP as chimera 4/EL2 (Table I), suggesting that these 3 residues act in concert to promote ATP agonism. The lack of activity of ATP at all concentrations tested at hP2Y$_4$-N178A and hP2Y$_4$-K179N receptors, together with the effects of the triple mutation, demonstrates that these residues have no role in ATP agonism in the P2Y$_4$ receptor.

Antagonist Effects of ATP at P2Y$_4$ Receptor Chimeras and Point Mutants

The antagonist activity of ATP was also tested with the hP2Y$_4$/rP2Y$_4$ chimeras and point mutants. In each case, the capacity of ATP to inhibit UTP-promoted intracellular Ca^{2+} mobilization was determined in 1321N1 cells expressing these receptor constructs. Cells were superfused with increasing concentrations of ATP in the presence of a concentration of UTP (1 μM) similar to the EC$_{50}$ values at the various P2Y$_4$ constructs (Table I). As demonstrated previously (17), ATP inhibited UTP-promoted Ca^{2+} mobilization in a concentration-dependent manner in cells expressing the hP2Y$_4$ receptor (Fig. 6). Similarly, ATP retained its antagonist properties at chimeras 2, 3, 5, and 6 (data not shown). These results are consistent with the observation that ATP failed to activate these same receptors, thus providing additional evidence that the receptor domains exchanged in these chimeras are not determinants of agonism/ antagonism of ATP at the P2Y$_4$ receptor. In contrast, ATP had no antagonist activity at chimeras 1 (Fig. 6) and 7 (data not shown). Thus, in addition to EL2, the NH$_2$ and COOH termini of the hP2Y$_4$ receptor also appear to contribute to the capacity of ATP to act as an antagonist.

The capacity of ATP to inhibit UTP-promoted intracellular Ca^{2+} mobilization also was determined in cells expressing the hP2Y$_4$ receptor point mutants. ATP antagonized UTP-promoted intracellular Ca^{2+} mobilization in cells expressing the wild type hP2Y$_4$ receptor as well as the hP2Y$_4$-N178A, hP2Y$_4$-K179N, and hP2Y$_4$-V183I point mutants (Fig. 6 and data not shown). In contrast, 300 μM ATP did not antagonize UTP-promoted Ca^{2+} mobilization in cells expressing the hP2Y$_4$-S177N mutant and inhibited ~50% of the UTP-promoted intracellular Ca^{2+} mobilization in cells expressing the hP2Y$_4$-R190L mutant (Fig. 6).

Cell Surface Expression of P2Y$_4$ Receptor Chimeras and Mutants

In face of the lack of a radioligand binding assay for quantification of surface expression of P2Y$_4$ receptors, we incorporated an HA-epitope tag at their NH$_2$ termini. This epitope tag was utilized to measure the relative cell surface expression of P2Y$_4$ receptors in intact 1321N1 cells as described under "Experimental Procedures." The level of expression of the various constructs varied by 3- to 4-fold. The majority of the receptors were expressed at about the same level as the hP2Y$_4$ receptor, whereas the rP2Y$_4$ receptor, chimeras 1/EL2 and 4/EL2, and the hP2Y$_4$-K179N point mutant were expressed at higher levels (Fig. 7). There was no correlation between the level of cell surface expression and the capacity of ATP to activate the receptor (*e.g.* the hP2Y$_4$-K179N receptor has one of the highest levels of expression but is not activated by ATP). Moreover, some of the chimeras with the highest apparent expression displayed the lowest EC$_{50}$ values for UTP promotion of Ca^{2+} mobilization. Thus, these data

suggest that differences in receptor expression did not account for the differences observed in responses to either UTP or ATP.

DISCUSSION

Because $hP2Y_4$ and $rP2Y_4$ receptors have high sequence identity (83%) yet display markedly different nucleotide selectivities, they represent an ideal receptor pair for investigating the molecular determinants of P2Y receptor agonism *versus* antagonism. To identify the region(s) of the receptor that determines the action of ATP, we constructed chimeric receptors in which consecutive regions of the $hP2Y_4$ receptor were replaced with the corresponding regions of the $rP2Y_4$ receptor and characterized their ability to promote Ca^{2+} mobilization in response to ATP. The data presented here demonstrate that the marked difference in agonist *versus* antagonist action of ATP at the $hP2Y_4$ and $rP2Y_4$ receptors primarily is the result of amino acid differences in their second extracellular loops, and to a lesser degree, their NH_2 termini.

All of the chimeras we generated (with the exception of chimera 4; see below) were activated fully by UTP with EC_{50} values that were very similar to the EC_{50} of UTP at the wild type $hP2Y_4$ receptor. These results suggest that there is little if any difference in affinity (and intrinsic efficacy) for UTP across a wide range of chimeric constructs. These results emphasize the power of a "gain-of-function" approach over the more widely applied loss-of-function studies utilized for other GPCRs, because it minimizes concerns that significant changes in the binding pocket have occurred due to aberrant folding of chimeric receptors. These data also suggest that the amino acids that regulate both the binding affinity and intrinsic efficacy of UTP are identical in both rat and human $P2Y_4$ receptors.

In contrast to UTP, ATP activated several of the chimeric constructs with variable potencies and efficacies. Because ATP binds to both the wild type rat and human homologues, but activates the rat receptor and antagonizes the human receptor, it is likely that both receptors contain the necessary amino acids to bind ATP. Thus, our data suggest that the changes in ATP potency and efficacy are not due to changes in binding affinity but rather arise from changes in the intrinsic activity of ATP. Moreover, observation of ATP agonism in the $hP2Y_4$ receptor with differing EC_{50} values in the different constructs suggests that multiple amino acids are involved in the conformational switch to the activated state and that these amino acids contribute to setting the level of intrinsic activity of ATP. That is, once the threshold is crossed that changes ATP from an antagonist to an agonist, further alterations in the protein likely change the intrinsic activity of ATP and not its affinity.

We observed a 10-fold decrease in the EC_{50} of UTP and a 50-fold decrease in the EC_{50} of ATP at chimera 4/EL2 compared with wild type $hP2Y_4$ and $rP2Y_4$ receptors. Interestingly, we did not observe similar decreases in the EC_{50} for UTP in the three individual EL2 point mutants, suggesting that the lower potencies of UTP at chimera 4/EL2 are due to the combined contribution of these three amino acids. It seems reasonable to propose that the decreases in potency of UTP and ATP at chimera 4/EL2 reflect a decrease in the intrinsic efficacy of both nucleotides such that higher concentrations of the nucleotides are required to achieve the same activity as in the wild type receptors.

Substitution of the $hP2Y_4$ NH_2 terminus with the corresponding region of the $rP2Y_4$ receptor (chimera 1) resulted in a receptor that minimally but reproducibly promoted an increase in intracellular $[Ca^{2+}]$ in response to high concentrations of ATP (Fig. 3*A*). In addition, ATP did not antagonize this receptor at the highest concentration tested (300 μM) (Fig. 6). We reasoned that replacing both EL2 and the NH_2 terminus of the $hP2Y_4$ receptor with the corresponding regions of the $rP2Y_4$ receptor might restore the EC_{50} values of ATP and UTP to those for the wild type $rP2Y_4$ receptor. Indeed, ATP and UTP activated chimera1/EL2 with higher potencies

compared with chimera 4 or 4/EL2. Moreover, adding the NH_2 terminus of the $rP2Y_4$ receptor to chimera 4/EL2 changed ATP from a partial agonist to an apparent full agonist. Thus, although the $rP2Y_4$ EL2 alone is sufficient to confer ATP agonist activity to the $hP2Y_4$ receptor, the $rP2Y_4$ NH_2 terminus appears to be an additional determinant that increases the intrinsic activity of ATP at the $rP2Y_4$ receptor. Even with the increase in potencies for ATP and UTP afforded by substitution of the $rP2Y_4$ NH_2 terminus into chimera 4/EL2, the EC_{50} values were still higher (especially for ATP) than those for the $rP2Y_4$ receptor. These data suggest that additional amino acids in the $rP2Y_4$ receptor function to increase the intrinsic efficacy of ATP. The identity of these other amino acids has not been pursued.

A cell surface RIA revealed that, compared with most of the receptor constructs, a subset of receptors was expressed at the cell surface at relatively high levels (Fig. 7). Interestingly, all of the receptors with increased expression contained an asparagine residue at position-179 instead of an aspartic acid (Fig. 1). Because both receptors have a threonine residue at position-181, an asparagine residue at position-179 creates a consensus *N*-linked glycosylation site. Indeed, Western blotting of the $rP2Y_4$ receptor revealed a diffuse band (data not shown) indicative of glycosylation compared with a single tight band for the $hP2Y_4$ receptor (which has no consensus glycosylation sites), suggesting that the site is utilized by the glycosylation machinery in 1321N1 cells. We considered whether glycosylation might change the ATP selectivity of the receptor; however, ATP had no agonist activity at the $hP2Y_4$-K179N receptor, which contains a glycosylation site and is expressed at higher levels on the cell surface. Moreover, there was no correlation between cell surface expression and the capacity of the receptor to be activated by ATP. These data are consistent with the interpretation that ATP agonist activity is mediated by amino acids in EL2 and not through changes in receptor expression.

Several studies have proposed attractive models for agonist activation and nucleotide docking within P2Y receptors. For example, Jiang *et al.* (24) suggested that positively charged amino acids near the exofacial side of TMs 3, 6, and 7 are important for ATP binding to the $hP2Y_1$ receptor, presumably through their interaction with the negatively charged phosphates of ATP. Several charged residues in the second and third extracellular loops of the $hP2Y_1$ receptor also have been implicated in ligand recognition (25). Erb *et al.* (26) reported that four positively charged amino acids in TMs 6 and 7 of the $hP2Y_2$ receptor play a role in agonist binding based on the loss of agonist potency. However, given the lack of a reliable binding assay for the P2Y receptor family, the results of these studies must be interpreted cautiously, because general conclusions were based on loss-of-function studies. In contrast, the observation that ATP does not activate the $hP2Y_4$ receptor provided an opportunity to make gain-of-function chimeras and mutants to correlate receptor function with specific receptor domains and amino acid residues. By reconstituting regions from the $rP2Y_4$ receptor into the $hP2Y_4$ receptor, the ability of ATP to function as an agonist was recapitulated in the background of the wild type $hP2Y_4$ receptor. These studies point to the $rP2Y_4$ receptor EL2 as a critical determinant for $P2Y_4$ agonist specificity.

It is well established that receptors for small ligands such as neurotransmitters and monoamines utilize transmembrane domains for ligand binding and activation (27,28). Although nucleotides are relatively small ligands, the P2Y receptors are more related to peptide receptors than they are to receptors for monoamines and neurotransmitters (29,30). The accepted models for ligand binding to GPCRs posit binding of endogenous peptide agonists in the extracellular loops and the exofacial regions of transmembrane domains, whereas the binding of non-peptide antagonists to the same receptors takes place deeper within the transmembrane domains (31). Here we add additional evidence that an extracellular loop (EL2) plays a critical role in the function of a GPCR ($P2Y_4$) most closely related to GPCRs for peptide ligands. The role of

extracellular loops in the activation of another nucleotide receptor (hP2Y$_1$ receptor) has been reported by Hoffman *et al.* (25).

Models for GPCR activity suggest that receptors spontaneously isomerize between inactive and active conformations and that the activated conformation associates with G proteins to promote intracellular signaling responses (32,33). According to these models, agonists exert their effects by preferentially binding to and stabilizing the activated conformation. Our data suggest that the amino acid differences found in the second extracellular loops (and, to a lesser extent, the NH$_2$ termini) of hP2Y$_4$ and rP2Y$_4$ receptors function to promote the active conformation upon ATP binding. Under this scenario, we hypothesize that the amino acids in the rP2Y$_4$ receptor EL2 (*i.e.* Asn-177, Ile-183, and Leu-190) utilize the binding energy of ATP to break the constraint within the inactive conformation and allow ATP to stabilize the active conformation and promote a subsequent signaling response.

To determine the potential validity of the preceding hypothesis and to visualize how ATP might bind to the P2Y$_4$ receptor, we manually docked ATP into the active site of a molecular model of the hP2Y$_4$ receptor (Fig. 8) based on the recent 2.4-Å structure of rhodopsin (34). The validity of this model, although illuminating, is tempered by the manual docking of ATP and by the fact that rhodopsin may not be a suitable template for generating molecular models of some GPCRs (35). Nonetheless, the results are interesting and are consistent with previous studies and the data presented here. For example, placement of the phosphate moiety of ATP in close proximity to TMs 6 and 7, as suggested by the mutagenesis experiments of Jiang *et al.* (24) and Erb *et al.* (26), positions the adenine base in an ideal position to interact with both EL2 and the NH$_2$ terminus. Also shown in Fig. 8 are the positions of the three amino acids identified in EL2 as being important in promoting the agonist activity of ATP. Interestingly, these three amino acids are widely separated in this preliminary model, and two of the three residues are far from the adenine ring, again consistent with our hypothesis that these residues are involved in conformational changes and not nucleotide binding. Lastly, this simple model suggests that the binding of ATP in the rat P2Y$_4$ receptor induces a conformational change that is transmitted through TMs 4 and/or 5, which then alters the conformation of the 2nd and/or 3rd intracellular loop and ultimately promotes activation of G$_q$.

Recent studies have revealed that mutations in a host of GPCRs result in constitutive activation (36–38). Receptors containing these mutations are thought to mimic the active conformation by adopting a structure capable of activating the G protein in the absence of agonists. These studies suggest that the wild type amino acids at these positions function to constrain the receptor in its inactive state and that mutation of these residues releases these constraints to allow the receptor to adopt an active conformation in the absence of agonists. Although most of these constitutively activating mutations are located in transmembrane domains, several of them, such as those found in angiotensin AT$_{1A}$, Ca^{2+} sensing, and thyrotropin receptors, are located within the extracellular loops (38–40). The location of constitutively activating mutations in the extracellular loops is consistent with our data, which demonstrate that residues within EL2 of the P2Y$_4$ receptor are involved in the switch to the active state. Thus, our data are also relevant to other GPCRs and suggest that, in addition to the more widely accepted role of TM domains, the extracellular loops also play an important role in activation.

In conclusion, we have used a gain-of-function approach with hP2Y$_4$/rP2Y$_4$ receptor chimeras to provide direct evidence that the second extracellular loop is the main determinant that confers the unique agonist/antagonist properties of ATP for these P2Y$_4$ receptor species homologues. The understanding of how nucleotides interact with P2Y$_4$ receptors to initiate signaling or antagonize functional responses could aid in the development of subtype-specific ligands, agents that will aid further studies of P2Y receptors as a whole.

References

1. Ralevic V, Burnstock G. Pharmacol Rev 1998;50:413–492. [PubMed: 9755289]

2. Harden, TK. Cardiovascular Biology of Purines. Burnstock, G.; Dobson, JG., Jr; Liang, BT.; Linden, J., editors. Kluwer Academic Publishers; Boston: 1998. p. 181-205.

3. North RA, Barnard EA. Curr Opin Neurobiol 1997;7:346–357. [PubMed: 9232809]

4. King BF, Townsend-Nicholson A, Burnstock G. Trends Pharmacol Sci 1998;19:506–514. [PubMed: 9871413]

5. Communi D, Govaerts C, Parmentier M, Boeynaems JM. J Biol Chem 1997;272:31969–31973. [PubMed: 9405388]

6. Communi D, Robaye B, Boeynaems JM. Br J Pharmacol 1999;128:1199–1206. [PubMed: 10578132]

7. Qi AD, Kennedy C, Harden TK, Nicholas RA. Br J Pharmacol 2001;132:318–326. [PubMed: 11156592]

8. Hollopeter G, Jantzen HM, Vincent D, Li G, England L, Ramakrishnan V, Yang RB, Nurden P, Nurden A, Julius D, Conley PB. Nature 2001;409:202–207. [PubMed: 11196645]

9. Zhang FL, Luo L, Gustafson E, Lachowicz J, Smith M, Qiao X, Liu YH, Chen G, Pramanik B, Laz TM, Palmer K, Bayne M, Monsma FJ Jr. J Biol Chem 2001;276:8608–8615. [PubMed: 11104774]

10. Takasaki J, Kamohara M, Saito T, Matsumoto M, Matsumoto S, Ohishi T, Soga T, Matsushime H, Furuichi K. Mol Pharmacol 2001;60:432–439. [PubMed: 11502873]

11. Foster CJ, Prosser DM, Agans JM, Zhai Y, Smith MD, Lachowicz JE, Zhang FL, Gustafson E, Monsma FJ Jr, Wiekowski MT, Abbondanzo SJ, Cook DN, Bayne ML, Lira SA, Chintala MS. J Clin Invest 2001;107:1591–1598. [PubMed: 11413167]

12. Communi D, Gonzalez NS, Detheux M, Brezillon S, Lannoy V, Parmentier M, Boeynaems JM. J Biol Chem 2001;276:41479–41485. [PubMed: 11546776]

13. Chambers JK, Macdonald LE, Sarau HM, Ames RS, Freeman K, Foley JJ, Zhu Y, McLaughlin MM, Murdock P, McMillan L, Trill J, Swift A, Aiyar N, Taylor P, Vawter L, Naheed S, Szekeres P, Hervieu G, Scott C, Watson JM, Murphy AJ, Duzic E, Klein C, Bergsma DJ, Wilson S, Livi GP. J Biol Chem 2000;275:10767–10771. [PubMed: 10753868]

14. Li Q, Olesky M, Palmer RK, Harden TK, Nicholas RA. Mol Pharmacol 1998;54:541–546. [PubMed: 9730913]

15. Zambon AC, Brunton LL, Barrett KE, Hughes RJ, Torres B, Insel PA. Mol Pharmacol 2001;60:26–35. [PubMed: 11408597]

16. Qi AD, Zambon AC, Insel PA, Nicholas RA. Mol Pharmacol 2001;60:1375–1382. [PubMed: 11723245]

17. Kennedy C, Qi AD, Herold CL, Harden TK, Nicholas RA. Mol Pharmacol 2000;57:926–931. [PubMed: 10779375]

18. Ho SN, Hunt HD, Horton RM, Pullen JK, Pease LR. Gene (Amst) 1989;77:51–59. [PubMed: 2744487]

19. Miller AD, Rosman GJ. BioTechniques 1989;7:980–982. 984–986, 989. [PubMed: 2631796]

20. Schachter JB, Boyer JL, Li Q, Nicholas RA, Harden TK. Br J Pharmacol 1997;122:1021–1024. [PubMed: 9401764]

21. Ali H, Richardson RM, Tomhave ED, DuBose RA, Haribabu B, Snyderman R. J Biol Chem 1994;269:24557–24563. [PubMed: 7929127]

22. Comstock, KE.; Watson, NF.; Olsen, JC. Methods in Molecular Biology: Recombinant Gene Expression Protocols. Tuan, R., editor. 62. Humana Press; Totowa, NJ: 1997. p. 207-222.

23. Schachter JB, Li Q, Boyer JL, Nicholas RA, Harden TK. Br J Pharmacol 1996;118:167–173. [PubMed: 8733591]

24. Jiang Q, Guo D, Lee BX, VanRhee AM, Kim YC, Nicholas RA, Harden TK, Jacobson KA. Mol Pharmacol 1997;52:499–507. [PubMed: 9281613]

25. Hoffmann C, Moro S, Nicholas RA, Harden TK, Jacobson KA. J Biol Chem 1999;274:14639–14647. [PubMed: 10329657]

26. Erb L, Garrad R, Wang Y, Quinn T, Turner JT, Weisman GA. J Biol Chem 1995;270:4185–4188. [PubMed: 7876172]

27. Dixon RAF, Sigal IS, Rands E, Register RB, Candelore MR, Blake AD, Strader CD. Nature 1987;326:73–77. [PubMed: 2881211]

28. Ostrowski J, Kjelsberg MA, Caron MG, Lefkowitz RJ. Annu Rev Pharmacol Toxicol 1992;32:167–183. [PubMed: 1318669]

29. Lustig KD, Shiau AK, Brake AJ, Julius D. Proc Natl Acad Sci U S A 1993;90:5113–5117. [PubMed: 7685114]

30. Van Rhee AM, Fischer B, Van Galen PJ, Jacobson KA. Drug Des Discov 1995;13:133–154. [PubMed: 8872457]

31. Berthold M, Bartfai T. Neurochem Res 1997;22:1023–1031. [PubMed: 9239758]

32. Samama P, Cotecchia S, Costa T, Lefkowitz RJ. J Biol Chem 1993;268:4625–4636. [PubMed: 8095262]

33. Kenakin T. Pharmacol Rev 1996;48:413–463. [PubMed: 8888308]

34. Palczewski K, Kumasaka T, Hori T, Behnke CA, Motoshima H, Fox BA, Le Trong I, Teller DC, Okada T, Stenkamp RE, Yamamoto M, Miyano M. Science 2000;289:739–745. [PubMed: 10926528]

35. Archer E, Maigret B, Escrieut C, Pradayrol L, Fourmy D. Trends Pharmacol Sci 2003;24:36–40. [PubMed: 12498729]

36. Cotecchia S, Exum S, Caron MG, Lefkowitz RJ. Proc Natl Acad Sci U S A 1990;87:2896–2900. [PubMed: 2158097]

37. Whistler JL, Gerber BO, Meng EC, Baranski TJ, von Zastrow M, Bourne HR. Traffic 2002;3:866–877. [PubMed: 12453150]

38. Parnot C, Miserey-Lenkei S, Bardin S, Corvol P, Clauser E. Trends Endocrinol Metab 2002;13:336–343. [PubMed: 12217490]

39. Parnot C, Bardin S, Miserey-Lenkei S, Guedin D, Corvol P, Clauser E. Proc Natl Acad Sci U S A 2000;97:7615–7620. [PubMed: 10852946]

40. Brown EM. Am J Med 1999;106:238–253. [PubMed: 10230755]

41. Hung LW, Wang IX, Nikaido K, Liu PQ, Ames GF, Kim SH. Nature 1998;396:703–707. [PubMed: 9872322]

The abbreviations used are

hP2Y receptor

human P2Y receptor, $hP2Y_4$ receptor, human $P2Y_4$ receptor

$rP2Y_4$ receptor

rat $P2Y_4$ receptor

IL2

second intracellular loop

EL2

second extracellular loop

TM

transmembrane domain

HA

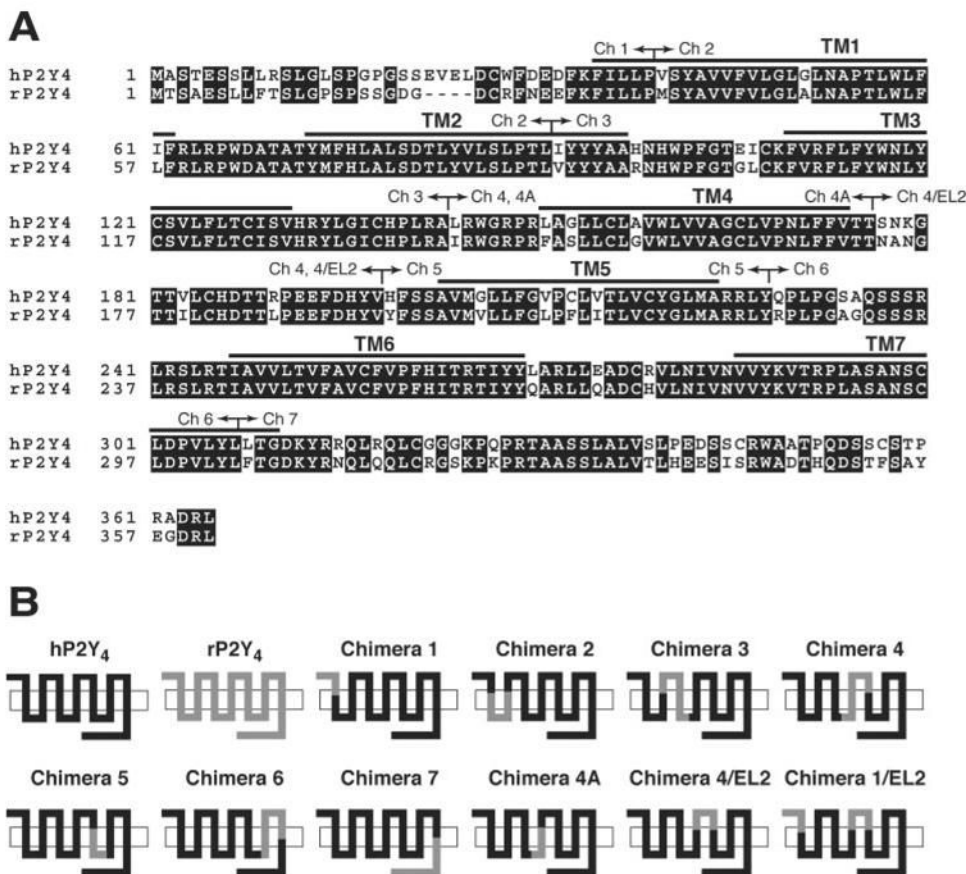hemagglutinin

GPCRs

G protein-coupled receptors

HBSS

Hanks' balanced salt solution

DMEM-H

Dulbecco's modified Eagle's medium with high glucose

AUC

area under the curve

A

B

Fig. 1. Alignment of hP2Y$_4$ and rP2Y$_4$ receptor sequences and schematic representation of hP2Y$_4$/rP2Y$_4$ chimeras

A, Boxshade (available on the World Wide Web) representation of a ClustalX alignment of human and rat P2Y$_4$ receptors. Gaps (−) were introduced to improve the alignment. The *arrows* represent the specific locations of sequence exchange in each chimera. *B*, schematic representation of receptor chimeras.
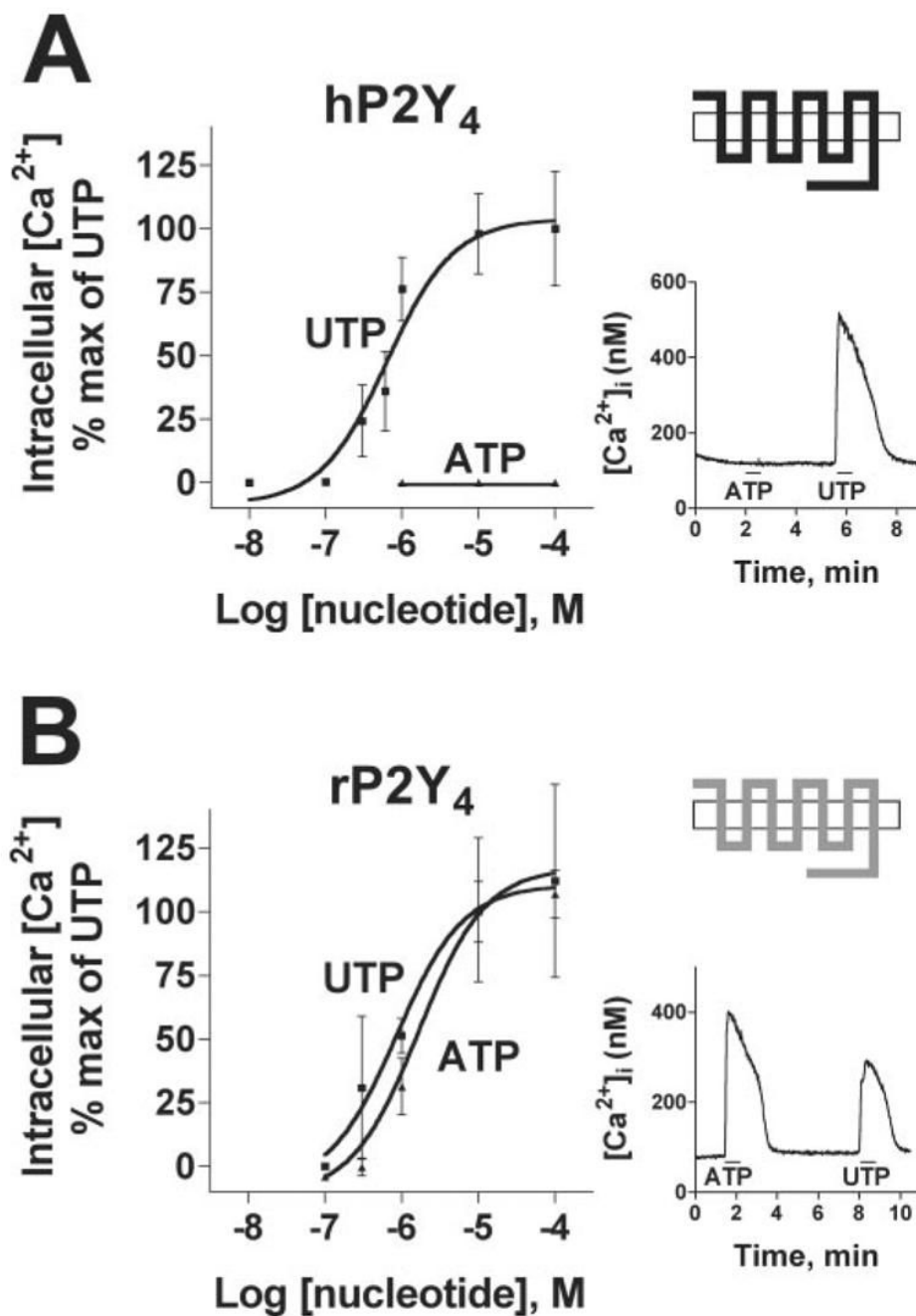
Fig. 2. Nucleotide-promoted intracellular Ca^{2+} mobilization in 1321N1 cells expressing either the hP2Y$_4$ (*A*) or rP2Y$_4$ (*B*) receptor

The *left panels* are concentration-response curves for UTP and ATP, and the *right panels* show Ca^{2+} traces to each nucleotide. To generate the concentration-response curves, individual coverslips of cells were exposed to a single concentration of nucleotide in buffer for 30 s. Traces of intracellular Ca^{2+} concentrations were recorded from 6–15 individual responding cells/coverslip and averaged. Data points represent the mean ± S.D. of the AUC from the averaged Ca^{2+} trace from a minimum of three coverslips and are presented as percentages of the maximal response to UTP. The Ca^{2+} traces in the *right panels* showing the responses to 100 μM ATP and 100 μM UTP are averages of at least six cells. Nucleotides were applied for

30 s as indicated by the *bars below the traces*. These results are representative of at least six similar experiments. The receptor schematics are identical to those in Fig. 1*B*.
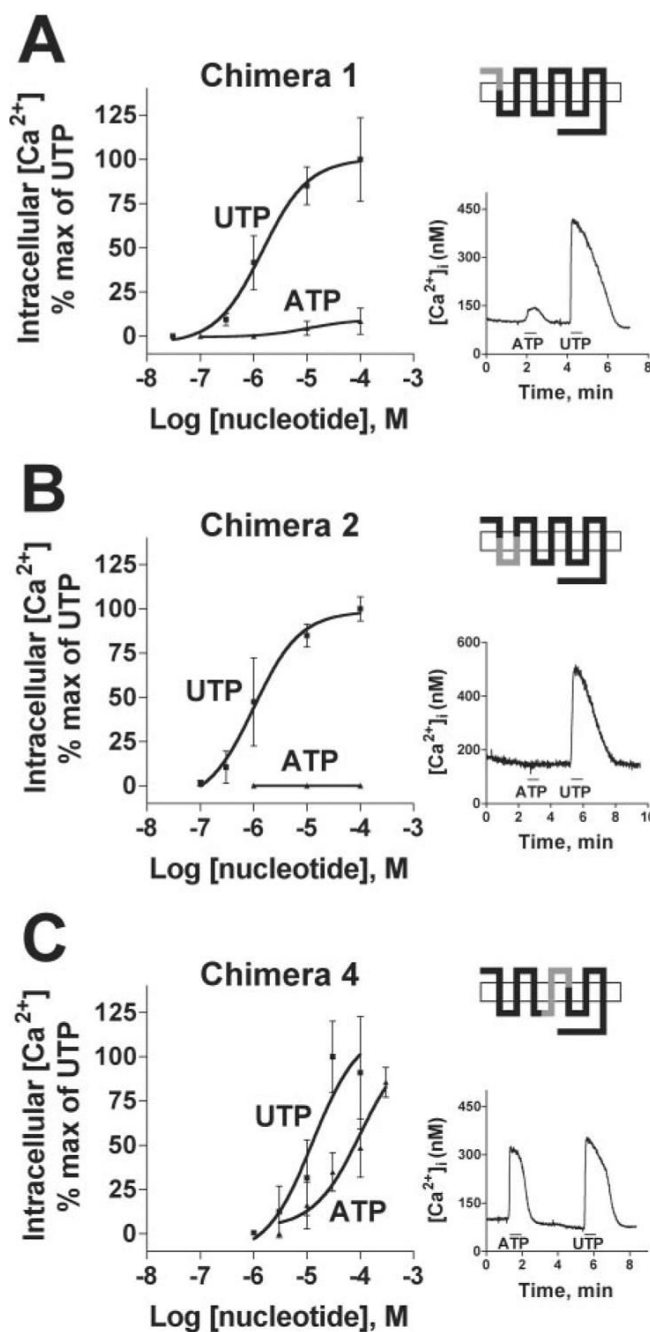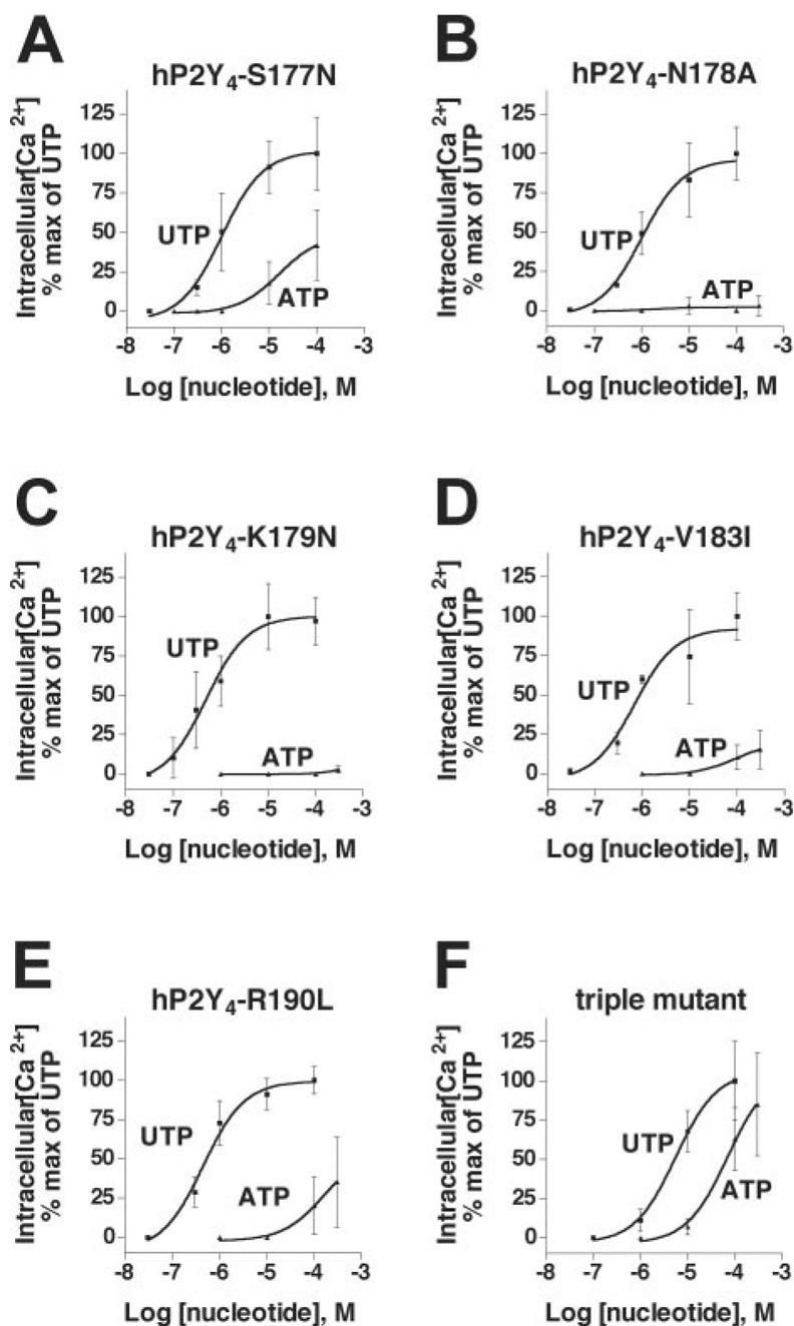
Fig. 3. Nucleotide-promoted intracellular Ca^{2+} mobilization in 1321N1 cells expressing hP2Y$_4$/rP2Y$_4$ receptor chimeras

A–E, the hP2Y$_4$ receptor with the single point mutations S177N, N178A, K179N, V183I, and R190L, respectively. F, the human P2Y$_4$ receptor with three point mutations, S177N, V183I, and R190L. See the legend to Fig. 2 for details. Chimeras 3, 5, 6, and 7 showed identical responses as chimera 2.
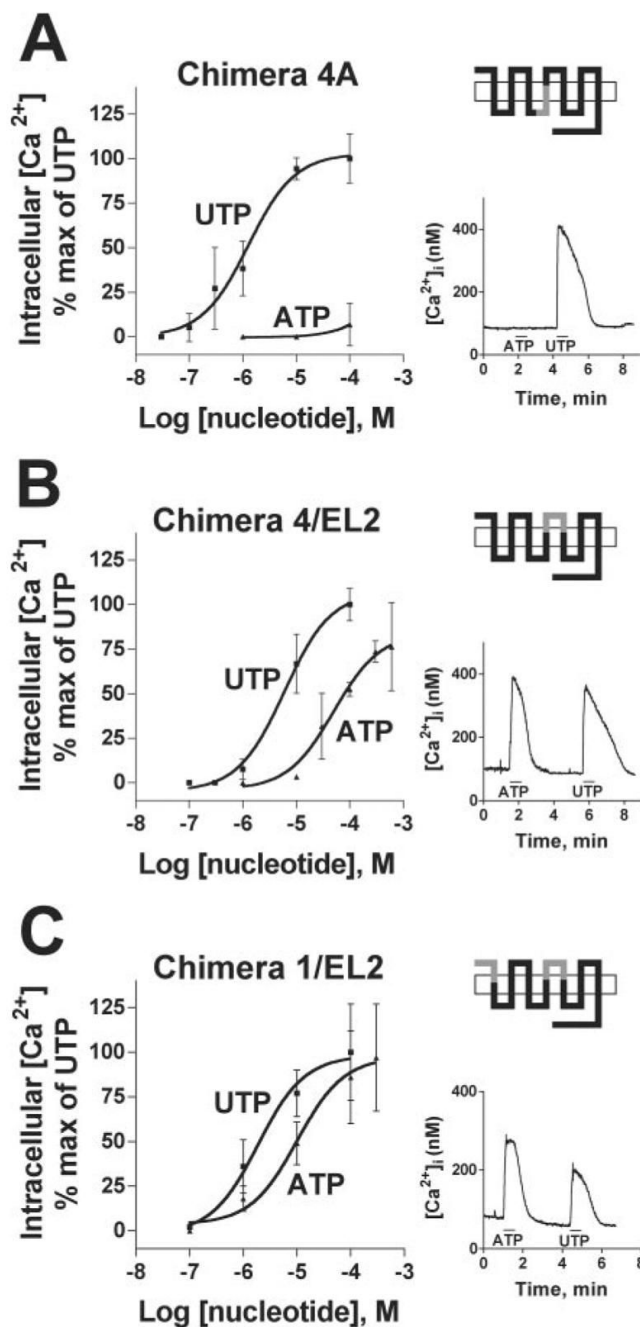
Fig. 4. Identification of the region in chimera 4 responsible for ATP-promoted intracellular Ca^{2+} mobilization

A, chimera 4A, the $hP2Y_4$ receptor containing IL2 and TM4 from the $rP2Y_4$ receptor. *B*, chimera 4/EL2, the $hP2Y_4$ receptor containing the EL2 from the $rP2Y_4$ receptor. *C*, chimera 1/EL2, the $hP2Y_4$ receptor containing the NH_2 terminus and EL2 from the $rP2Y_4$ receptor. See the legend to Fig. 2 for details.

Fig. 5. Nucleotide-promoted intracellular Ca^{2+} mobilization in 1321N1 cells expressing single point mutants within EL2 of the hP2Y$_4$ receptor

A, chimera 1, the hP2Y$_4$ receptor containing the NH_2 terminus from the rP2Y$_4$ receptor. *B*, chimera 2, the hP2Y$_4$ receptor containing TM1, IL1, and TM2 from the rP2Y$_4$ receptor. *C*, chimera 4, the hP2Y$_4$ receptor containing IL2, TM4, and EL2 from the rP2Y$_4$ receptor. The concentration-response curves from the five individual point mutants of the hP2Y$_4$ receptor and a receptor containing the S177N, V183I, and R190L mutations (triple mutant) are shown.
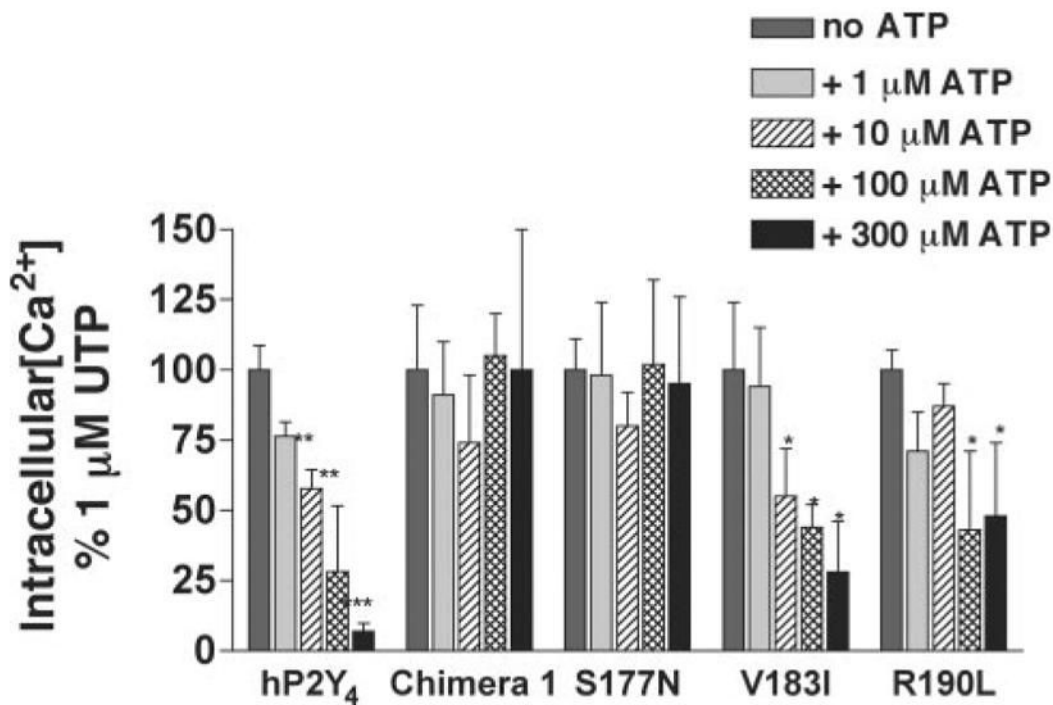
Fig. 6. ATP antagonism of UTP-promoted intracellular Ca^{2+} mobilization in 1321N1 cells expressing either the hP2Y$_4$ receptor chimeras and point mutants
Single coverslips of cells were exposed to either 1 μM UTP alone or 1 μM UTP plus the indicated concentration of ATP for 30 s. Traces of intracellular Ca^{2+} concentrations were recorded from 6–15 individual responding cells/coverslip and averaged. Each *bar* represents the mean ± S.D. of the AUC from the averaged Ca^{2+} trace from a minimum of three coverslips and is presented as a percentage of the maximal response to 1 μM UTP. *, $p < 0.05$; **, $p < 0.01$; ***, $p < 0.001$ relative to the response of 1 μM UTP.
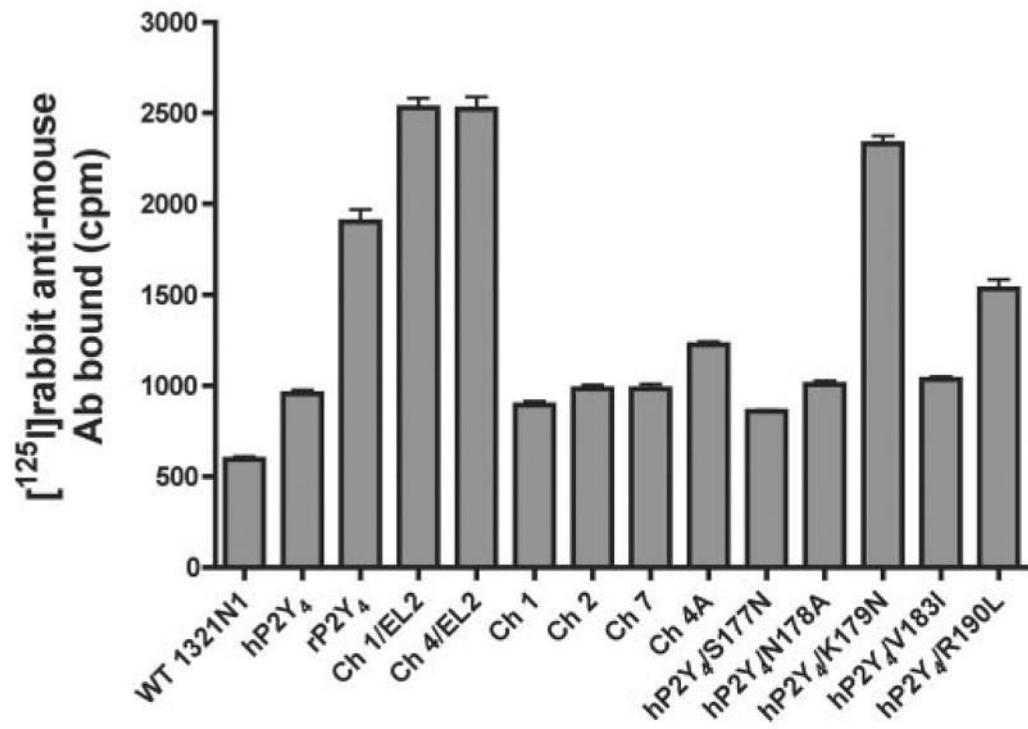
Fig. 7. Cell surface RIA analysis
Cell surface expression of various receptor constructs was quantitated as described under
"Experimental Procedures." The values represent the average of three separate determinations.
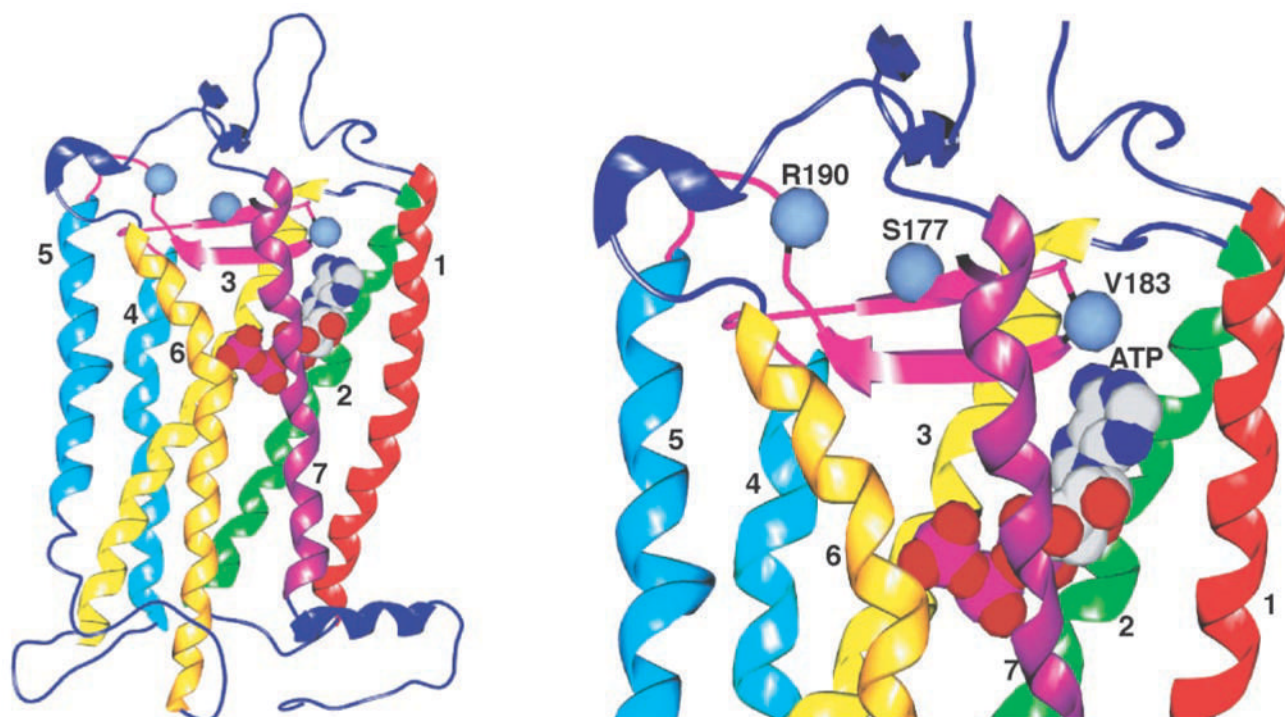
Fig. 8. Manual docking of ATP into a molecular model of the P2Y$_4$ receptor

The molecular model of the hP2Y$_4$ receptor was developed with the program InsightII based on the crystal structure of rhodopsin (1F88 (34)). The coordinates for ATP were obtained from the structure of the ATP-binding subunit of Histidine Permease (1B0U (41)). The ATP molecule was docked manually into the P2Y$_4$ model so that its triphosphate moiety was in close proximity to the exofacial sides of TMs 6 and 7 as suggested by Jiang *et al.* (24) and Erb *et al.* (26). These images were generated with the program Spock (available on the world wide web).

Table I

Potencies of UTP and ATP for mobilization of intracellular [Ca^{2+}] at the various P2Y$_4$ receptors described in this study

Dose-response curves were generated as described under "Experimental Procedures." EC$_{50}$ values (μM) are presented as mean values ± S.D. for wild type hP2Y$_4$ and rP2Y$_4$ receptors ($n \geq 5$) or as values (95% confidence intervals) calculated by nonlinear regression for all of the chimeric and mutant receptors.

Receptor	UTP	ATP
hP2Y$_4$	0.53 ± 0.22 ($n = 5$)	NE[a] ($n = 7$)
rP2Y$_4$	0.60 ± 0.22 ($n = 6$)	0.89 ± 0.46 ($n = 7$)
Chimera 1	1.5 (0.64–3.3)	ND[b]
Chimera 2	1.0 (0.47–2.2)	NE
Chimera 3	0.66 (0.17–2.5)	NE
Chimera 4	13 (3.1–54)	95 (28–320)
Chimera 5	0.9 (0.3–2.7)	NE
Chimera 6	0.55 (0.16–3.5)	NE
Chimera 7	0.80 (0.22–2.9)	NE
Chimera 4A	1.3 (0.58–2.9)	NE
Chimera 4/EL2	6.0 (3.4–11)	51 (19–140)
Chimera 1/EL2	1.9 (0.50–7.2)	12 (2.4–58)
hP2Y$_4$ S177N	1.0 (0.38–2.7)	ND
hP2Y$_4$ N178A	1.0 (0.40–2.6)	NE
hP2Y$_4$ K179N	0.50 (0.20–1.2)	NE
hP2Y$_4$ V183I	0.69 (0.24–2.0)	ND
hP2Y$_4$ R190L	0.45 (0.25–0.81)	ND
Triple mutant	5.6 (2.1–16)	48 (7.2–320)

[a]NE, no effect.

[b]ND, not determined; the response to ATP did not reach maximum at the highest concentration tested (300 μM).